sciendo

Summer–winter contrast in carbon isotope and elemental composition of total suspended particulate matter in the urban atmosphere of Krakow, Southern Poland

Miroslaw Zimnoch ,
Filip Morawski,
Tadeusz Kuc,
Lucyna Samek ,
Jakub Bartyzel ,
Zbigniew Gorczyca ,
Alicja Skiba,
Kazimierz Rozanski

Abstract. The city of Krakow located in southern Poland ranks among the most polluted urban agglomerations in Europe. There are persisting controversies with respect to impact of different pollution sources operating in Krakow agglomeration on air quality within the city. The presented pilot study was aimed at exploring the possibilities offered by elemental and carbon isotope composition of total suspended particulate matter (TSPM) for better characterization of its sources in Krakow atmosphere. The analyses of carbon isotope composition of total carbon in the investigated TSPM samples were supplemented by parallel analyses of radiocarbon content in atmospheric carbon dioxide (CO_2). This study revealed large seasonal variability of carbon isotope composition in the analysed TSPM samples. This large variability reflects seasonally varying contribution of different sources of fossil and modern carbon to the TSPM pool. The elemental composition of TSPM also reveals distinct seasonal variability of the analysed elements, reflecting varying mixture of natural and anthropogenic sources of those elements. A linear relationship between the fossil carbon load in the TSPM samples and the fossil carbon load in the atmospheric CO_2 was found, pointing to the presence of additional source of anthropogenic carbonaceous particles not associated with burning of fossil fuels. Wearing of tyres and asphalt pavement is most probably the main source of such particles.

Keywords: Air pollution • Suspended particle matter • Carbon isotopes • Elemental composition • Pollution sources

M. Zimnoch✉, F. Morawski, T. Kuc, L. Samek,
J. Bartyzel, Z. Gorczyca, A. Skiba, K. Rozanski
Faculty of Physics and Applied Computer Science
AGH University of Science and Technology
Al. Mickiewicza 30, 30-059 Krakow, Poland
E-mail: zimnoch@agh.edu.pl

Introduction

Deterioration of air quality in urban agglomerations is a growing problem of global significance (e.g. [1, 2]). This spurs research towards better understanding of parameters controlling air quality in urban environment, such as different sources of particulate matter and gaseous contaminants, spatial and temporal variability of their emissions and impact of the dynamics of urban atmosphere on the observed concentration of atmospheric aerosols (e.g. [3–5]).

Analyses of elemental and chemical composition of suspended particulate matter (SPM) are used to track sources and physico-chemical transformations of atmospheric aerosols in urban environment. Although initially only total SPM (TSPM) was studied, soon major efforts were directed towards comprehensive characterization of specific size fractions of SPM: PM_{10}, $PM_{2.5}$ and $PM_{1.0}$ (e.g. [6–8]). Organic matter, sulphates, nitrates, ammonia, elemental carbon, mineral dust and sodium chloride are typically present in SPM in $\mu g \cdot m^{-3}$ range, whereas elements such as Ti, As, Cr, Cu, Zn, Br and Pb occur usually in trace (in $ng \cdot m^{-3}$) amounts.

Traffic-related elements present in SPM may come from car exhaust (Cu, Zn, Fe, Br and Pb), wearing of brake pads and shoes (Cu) or tyres (Zn) and street dust resuspended by traffic (Fe, Mn, Si, Ca, Na, Mg, Al and K) [9–11]. The indicators of oil combustion are Ni and V [10]. Soil particles contain Al, Si, Ca, Ti, Fe, K and some others. These elements are also typical for fly ash from coal combustion [10]. The urban emission sources are characterized by the presence of Cl, S, Fe, Br and Zn [10–12]. The emissions from sources related to steel production typically contain Fe, Mn and Zn.

Chemical and elemental composition of SPM is often used to classify the sources of atmospheric aerosols. Positive matrix factorization (PMF) is a preferable method used for this purpose [13]. It links the measured concentrations of elements and chemical compounds in SPM with their potential sources present in the urban environment. For instance, in a study conducted during 2014–2015, Samek *et al.* characterized the sources of $PM_{2.5}$ fraction of SPM present in Krakow atmosphere and their seasonal variability using this method and found that six source categories can be identified: secondary sulphate, secondary nitrate, combustion, biomass burning, steel industry/soil dust and traffic [14].

Major component of SPM in urban atmosphere is carbon. The reservoir of total carbon (TC) in atmospheric aerosols consists of elemental carbon (EC) and organic carbon (OC). EC is produced by incomplete combustion of fossil and biomass fuels in an oxygen-poor environment [15]. The OC pool is composed of hundreds of chemical constituents belonging to many compound classes and it is usually separated into two fractions: primary and secondary OCs. Primary OC sources are related to fossil-fuel combustion, biomass burning and bio-aerosol emissions. The secondary OC pool in SPM originates in physico-chemical transformations of carbonaceous pollutants present in the atmosphere.

Carbon isotope analysis of carbonaceous fraction of SPM became an important tool for apportionment of carbon sources. Number of researches used ^{13}C isotope signatures of carbonaceous aerosols as a marker of carbon origin [16, 17]. Radiocarbon content in carbonaceous aerosols was used as a tool to quantify the contribution of carbon originating from combustion of fossil fuels [18, 19]. Initially, radiocarbon content in TC fraction has been measured. Later on, with the development of methods for separation of EC and OC fraction it was possible to quantify separately both carbon types in different size fractions of SPM (e.g. [20–23]). Recently, attempts have been made to combine ^{13}C and ^{14}C isotope ratios measured in carbonaceous aerosols in source apportionment of airborne particulate matter in urban and rural sites in Lithuania [24].

The city of Krakow, located in southern Poland, ranks among the most polluted urban agglomerations in Europe. Several pollution sources are responsible for high levels of air pollution in the city. Steel, cement and ceramic industries as well as heat and power plants are located in Krakow. The important sources of pollution are related to burning of coal and biomass as well as to traffic. Less important in the budget is soil and street dust [25, 26].

The evolution of PM_{10} concentration during the period 2004–2017 (annual and seasonal means) recorded at the station belonging to air quality monitoring network in Krakow is shown in Fig. 1a.
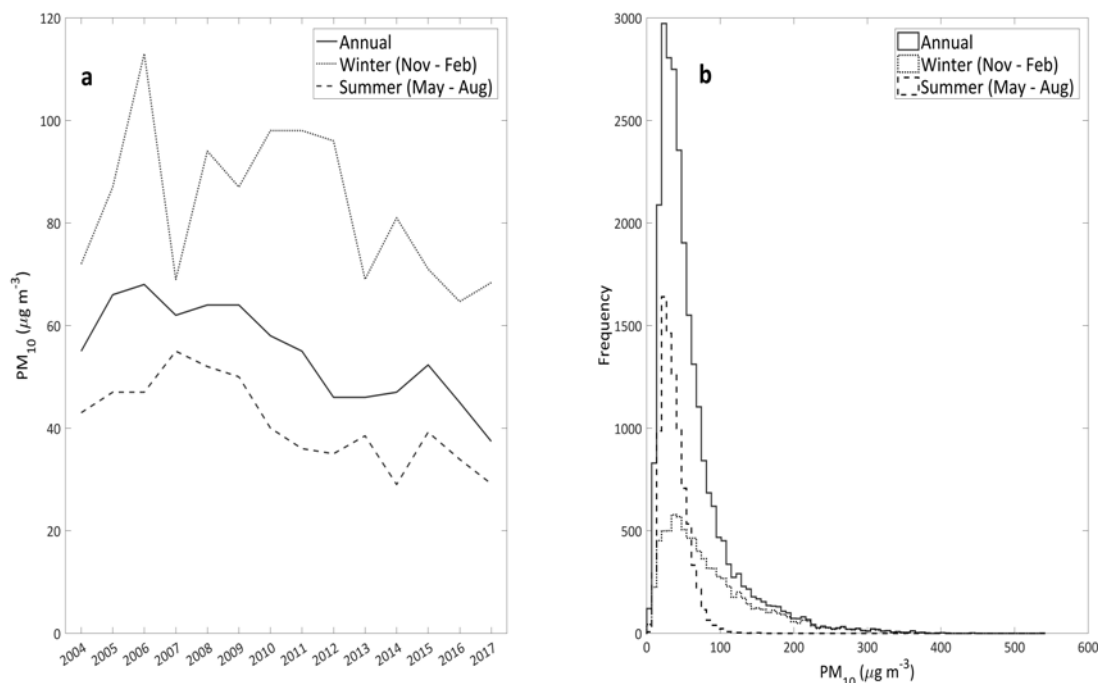
Fig. 1. (a) Evolution of mean PM_{10} concentrations in the urban atmosphere of Krakow during the period 2004–2017. Shown are annual and seasonal (summer and winter) median concentrations of PM_{10} recorded at the station belonging to air quality monitoring network in Krakow operated by State Inspectorate of Environmental Protection. Source: www.krakow.pios.gov.pl. For location of the station, see Fig. 2. (b) Annual and seasonal frequency distributions of hourly means of PM_{10} concentration at the station calculated during 2015.
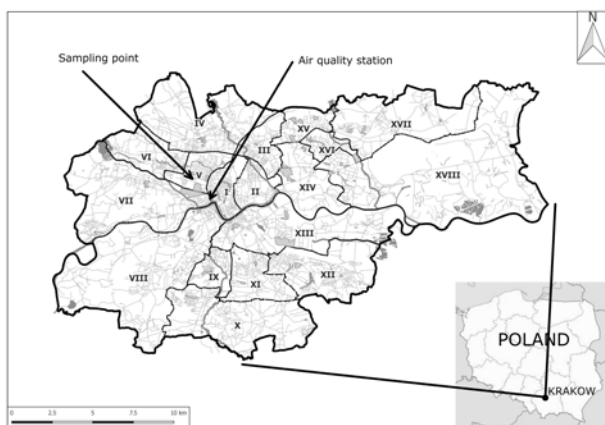
Fig. 2. The study area. Krakow agglomeration border is marked by a solid line. District I represents the oldest part of the city. Site where TSPM samples were collected is labelled as 'sampling point'. Monitoring of carbon isotope composition of atmospheric CO_2 was conducted at the same location. The station of air quality monitoring network in Krakow which PM_{10} data for 2005–2017 are presented in Fig. 1 and is labelled as 'air quality station'.

The station is located approximately 2 km south-east from the site where samples of TSPM analysed in the framework of this pilot study were collected (cf. Fig. 2) and it monitors mostly traffic-related pollution. Apparent is strong seasonality of PM_{10} fraction in the local atmosphere, with median concentrations during winter months (November–February) exceeding the corresponding median concentrations during summer months (May–August) in the given year by a factor of 1.6–3.1. It is also apparent from Fig. 1a that PM_{10} levels, particularly during winter time, exceeded the guidelines of WHO and of EU Directive set at 50 $\mu g \cdot m^{-3}$ [27, 28]. Although there are substantial inter-annual variations of median values, particularly visible for winter period, it is also apparent that there is a slight decreasing trend of approximately 1.6 $\mu g \cdot m^{-3} \cdot year^{-1}$ for the annual means in all three time series as shown in Fig. 1a. State Inspectorate of Environmental Protection responsible for air quality monitoring network in Krakow reported that yearly mean concentration of PM_{10} fraction in Krakow atmosphere (average of PM_{10} data originating from six stations distributed throughout the city) decreased from approximately 67 $\mu g \cdot m^{-3}$ in 2005 to 51 $\mu g \cdot m^{-3}$ in 2013, i.e. 1.23 $\mu g \cdot m^{-3} \cdot year^{-1}$ [29], which is similar to the linear trend of data shown in Fig. 1a. Figure 1b shows frequency distributions of hourly mean PM_{10} concentrations recorded at the station during entire 2015. Large differences in seasonal spectra are seen. Whereas the distribution of hourly means during summer months is almost symmetric, winter spectrum has a long tail extending to high PM_{10} concentrations. This long tail has its roots mostly in the dynamics of the local atmosphere (cf. discussion later). Also, there are additional sources of SPM during winter period (burning of coal and wood in individual households for heating purposes).

There is an ongoing discussion with respect to significance of different sources of particulate matter in the urban atmosphere of Krakow, such as low- and high-elevation emissions related to burning of fossil fuels (mostly coal) and biomass for heating purposes, traffic, resuspension of street dust and some others. The presented work was aimed at exploring the possibilities offered by elemental and carbon isotope composition of SPM for better characterization of its sources in Krakow atmosphere, with the focus on seasonal changes in the character and intensity of those sources. Also, due to the fact that analysed archive material covered the period 2004–2010, it was possible to draw some conclusions with respect to long-term trends in fossil-fuel-derived fraction of TC reservoir in the analysed samples of SPM.

Study area

Krakow ranks fourth among largest cities in Poland. With nearly 1 million inhabitants, rapidly growing car traffic and significant industrial activities, Krakow agglomeration represents typical urban environment in Eastern Europe. The city covers the area of ca. 327 km^2 and it is located in the Vistula river valley oriented in this region along the east-west axis. In the south, the city borders a hilly terrain, while in the north it opens towards flat upland area. With prevailing westerly circulation, Krakow region is under substantial influence of large coal mining and industrial district (Upper Silesia) located approximately 60 km west of the city. The characteristic features of the local climate are generally weak winds (annual average around 2.7 ms^{-1}) and frequent inversions, sometimes extending over several days, particularly during winter season. These factors favour accumulation of particulate matter and gaseous pollutants in the city's atmosphere.

Relatively large amounts of coal are burnt annually within the limits of Krakow agglomeration. Coal is burnt mostly in individual households for heating purposes. Although there is a gradual shift from coal to gas, the recent count revealed that approximately 23 000 of coal-burning ovens were still in operation in Krakow in 2016 [30]. The number of cars registered in the city has increased from approximately 335 000 in 2008 to 448 000 in 2016 [31]. The car fleet is still rather old, with relatively large number of diesel cars (ca. 27%), significant part of it without catalyst and particle filter. Substantial number of cars (ca. 11%) is powered by liquefied petroleum gas (LPG).

The samples of TSPM were collected on the University campus situated in the western sector of the city (50°04'N, 19°55'E, 220 m above sea level), bordering recreation and sports grounds. The air intake was placed on the roof of the faculty building, approximately 20 m above the local ground. Monitoring of carbon isotope composition of atmospheric carbon dioxide (CO_2) was conducted at the same location.

Materials and methods

Samples of TSPM investigated in the framework of this pilot study were collected as a part of long-

Table 1. Samples of TSPM collected in Krakow and investigated in the presented study

Sample code*	Sample collection period	Mass of TSPM sample** [mg]
C-1-S	09.08.2004 – 19.08.2004	16.83
C-2-W	25.01.2005 – 08.02.2005	32.28
C-3-S	30.05.2005 – 22.06.2005	14.10
C-4-W	27.01.2006 – 06.02.2006	33.21
C-5-S	05.07.2006 – 13.07.2006	4.89
C-6-W	08.02.2007 – 13.02.2007	8.79
C-7-S	13.06.2007 – 18.06.2007	10.24
C-8-W	15.02.2008 – 18.02.2008	9.82
C-9-S	08.07.2008 – 23.07.2008	4.55
C-10-W	08.01.2009 – 15.01.2009	13.63
C-11-S	08.05.2009 – 17.06.2009	9.65
C-12-W	14.01.2010 – 08.02.2010	23.78

*Letters W and S signify winter and summer periods, respectively. **Standard uncertainty of the reported masses is in the order of 0.01 mg.

-term monitoring of ^{222}Rn activity in near-ground atmosphere of the city. The instrument in use (radon monitor) employs an indirect method of ^{222}Rn detection via its radioactive progenies deposited on filter [32]. TSPM was sampled continuously on quartz filters (Whatman, QMA, diameter 47 mm, flow rate of ca. 0.7/1.1 m^3·h^{-1}). Filters were replaced when the flow rate dropped by more than 20%. Periods of sampling varied from 3 days to 23 days. The used filters were placed in plastic sheets with zip tightly closed and stored under controlled conditions.

For this pilot study, six pairs of TSPM samples collected during the period 2004–2010, representing summer and winter conditions, respectively, were selected (cf. Table 1). The selected TSPM samples were analysed in three steps. First, the mass of deposited particulate matter was determined gravimetrically on standardized portions of the filters (circles of the diameter of 34 mm cut-out of original filter material). Then, the concentration of selected elements (Cl, K, Ca, Ti, Cr, Mn, Fe, Cu, Zn, As, Br, Rb, Sr and Pb) was determined using energy dispersive X-ray fluorescence (EDXRF) technique. Finally, the TC present in the samples was converted to CO_2 in which composition of carbon isotopes (^{13}C and ^{14}C contents) was analysed.

Multi-element analyses were performed using multifunctional energy-dispersive X-ray fluorescence spectrometer [33]. It consists of a microbeam X-ray fluorescence spectrometer with capillary X-ray optics, broad X-ray beam from Mo secondary target for XRF analysis of bulk samples and a total reflection X-ray set-up. The Mo tube is the source of X-rays. The tube has the power of 2 kW. The excited X-rays were detected by the Si(Li) detector with the resolution of 170 eV for the line of 5.9 keV. The spectrometer was calibrated using thin-film standards (Micromatter, USA). Calibration was verified by the analysis of NIST Standard Reference Material 2783 – Air Particulate Matter on filter media. The XRF spectra were quantitatively analysed with the use of the QXAS package [34]. A blank filter correction

has been made by substracting the concentrations of analysed elements measured for clean filters from the concentrations obtained for the analysed TSPM samples. The corrections were in the range from approximately 1% (Fe) to 26% (Ca) of the measured concentrations.

For conversion of the TC pool present in TSPM samples to CO_2, sealed-tube technique was adopted [35]. Standardized portions of the analysed filters were cut into pieces and placed in pre-baked quartz combustion tubes. CuO and silver wool were added to the tubes which were then evacuated and flame-sealed. The sealed tubes were placed in muffle oven and baked for 3 h at 850°C. In this way, carbon present on the analysed filters was quantitatively converted to CO_2. The obtained CO_2 gas was then purified cryogenically in a dedicated vacuum extraction line. The pressure of the extracted CO_2 was measured in a calibrated volume of the extraction line and the mass of carbon in the analysed TSPM sample was calculated. The CO_2 gas was then split into two aliquots: one for accelerator mass spectrometry (AMS) ^{14}C and the other for isotope-ratio mass spectrometry (IRMS) ^{13}C analyses, respectively. The ^{14}C analyses were conducted in Poznan Radiocarbon AMS Laboratory (www.radiocarbon.pl). The ^{13}C analyses were conducted at Mass Spectrometry Laboratory of the Faculty of Physics and Applied Computer Science (AGH, Krakow) using delta S isotope ratio mass spectrometer, following standard protocols. Typical uncertainty of carbon isotope analyses was in the order of 0.4% of modern carbon for ^{14}C and 0.1‰ for δ^{13}C.

The ^{14}C and ^{13}C analyses conducted in the framework of this pilot study were performed on archive filters which were not pre-baked. Therefore, the experiments have been carried out to quantify the level of possible carbonaceous blank on the filters. Eight filters randomly selected from a pack of new filters which were used for ^{222}Rn monitoring were processed using the above-outlined procedure, and the volume of the evolved CO_2 was measured and converted to the mass of carbon. The average mass of carbon on the filters subject to this procedure was 0.08 ± 0.04 mg. The ^{13}C analyses of the evolved CO_2 yield the mean δ^{13}C value of (–23.1 ± 0.4)‰, confirming organic origin of carbonaceous blank. If one assumes the worst-case scenario in which the carbonaceous blank consists exclusively of modern carbon and the mass of carbon on a filter is low (such as for samples C-5-S and C-9-S, cf. Table 1), the resulting correction for the per cent fraction of fossil carbon in the TC present in the analysed samples of TSPM (FF$_{TSPM}$; cf. Eq. (3)) would be substantially lower than 1%. Therefore, no additional correction for the presence of carbonaceous blank was introduced to the calculated values of FF$_{TSPM}$ reported in Table 3.

If one assumes that the total mass of carbon (m_{TOT}) in the analysed samples of TSPM consists of only two fractions, i.e. the mass of carbon originating from combustion of fossil fuels (m_{FF}) and the mass of modern carbon originating from burning of biomass (mostly wood) and from biospheric emissions (m_{MOD}), the following mass and ^{14}C isotope balance can be formulated:

(1) $$m_{\mathrm{TOT}} = m_{\mathrm{MOD}} + m_{\mathrm{FF}}$$

(2) $$^{14}R_{\mathrm{TOT}}\, m_{\mathrm{TOT}} = {}^{14}R_{\mathrm{MOD}}\, m_{\mathrm{MOD}} + {}^{14}R_{\mathrm{FF}}\, m_{\mathrm{FF}}$$

where R_{TOT}, R_{MOD} and R_{FF} signify $^{14}C/^{12}C$ isotope ratios of corresponding mass balance components. Since fossil fuels are devoid of radiocarbon, it follows that $R_{\mathrm{FF}} = 0$. From Eqs. (1) and (2), the following expression for per cent fraction of fossil carbon in the TC present in the analysed samples of TSPM can be derived:

(3) $$\mathrm{FF_{TSPM}}(\%) = \frac{m_{\mathrm{FF}}}{m_{\mathrm{TOT}}} \cdot 100 = \left(1 - \frac{R_{\mathrm{TOT}}}{R_{\mathrm{MOD}}}\right) \cdot 100$$

The $^{14}C/^{12}C$ isotope ratios are usually expressed as per cent of modern carbon which is defined as 95% of the specific activity of internationally accepted standard NBS Oxalic Acid (Ox1) in the year 1950 [36]. It closely resembles the ^{14}C content of carbon in plants growing around 1890 in fossil–CO_2-free environment. At present, since burnt biomass contains measurable fraction of bomb-derived ^{14}C, it was assumed in Eq. (3) that R_{MOD} is $(110 \pm 5)\%$ of modern carbon.

The reservoir of TC in TSPM samples may also contain carbon devoid of ^{14}C which is associated with the presence of mineral dust in atmospheric aerosols. This carbon is mostly in the form of carbonates (Ca or Mg). Such carbonates, if present in the analysed TSPM samples, will be decomposed during the sealed-tube combustion process and will influence the carbon isotope analyses of TC. Since in the presented study the concentration of Ca in the analysed TSPM samples was measured using X-ray fluorescence (XRF) technique, appropriate corrections of the measured $^{14}C/^{12}C$ and $^{13}C/^{12}C$ ratios could be made (see the next section). Although Mg content was not analysed, we consider the correction based exclusively on Ca content acceptable for the purposes of this study because Ca is incorporated also in sulphates, present in the analysed TSPM samples, thus potentially compensating for unknown reservoir of magnesium carbonate. Appropriate corrections of ^{14}C content (R_{TOT}) and $\delta^{13}C$ values of the analysed TSPM samples were made based on the fraction of carbon in the TC reservoir, calculated for each analysed sample on the basis of Ca concentration, assuming that calcium carbonate is devoid of ^{14}C and its $\delta^{13}C$ value is zero (primary carbonate of marine origin).

In parallel to TSPM samples collected on filters, the levels of ^{14}C in CO_2 present in Krakow atmosphere during the time span covered by analysed filters were also measured as a part of long-term monitoring programme of atmospheric CO_2 [37]. Weekly composite samples of atmospheric CO_2 were collected using the method, based on the sorption of CO_2 on molecular sieve [38]. The ^{14}C content in the collected CO_2 was measured using benzene synthesis followed by liquid scintillation spectrometry [39]. Applying isotope mass balance similar to that described by Eqs. (1) and (2), the following expression for percentage contribution of fossil-fuel-derived component in atmospheric CO_2 can be derived [40]:

(4) $$\mathrm{FF_{CO2}}(\%) = \frac{C_{ff}}{C_{\mathrm{tot}}} \cdot 100 = \frac{\Delta^{14}C_{bg} - \Delta^{14}C_{\mathrm{tot}}}{\Delta^{14}C_{bg} + 1000} \cdot 100$$

where C_{tot} and C_{ff} stand for total and fossil-fuel-derived mixing ratio of CO_2 in the local atmosphere, respectively. The concentration of ^{14}C in the regional background ($\Delta^{14}C_{bg}$) and the local atmospheric CO_2 ($\Delta^{14}C_{\mathrm{tot}}$) is expressed as per mil deviations from the NBS oxalic acid standard, following the generally accepted notation [36]. As a regional background, $\Delta^{14}CO_2$ measurements performed at the High Alpine Research Station Jungfraujoch (Swiss Alps, 46°33'N, 7°59'E, 3450 m a.s.l.) by the Institute of Environmental Physics, University of Heidelberg, Germany were adopted [41]. For the 2004–2009 period, the average contribution of the fossil-fuel-derived CO_2 to the overall CO_2 burden of the local atmosphere in Krakow, derived using Eq. (4), was approximately 3.4% [42].

Results and discussion

Elemental analysis

Mean concentrations of the selected elements in the analysed TSPM samples representing summer (S) and winter (W) period are reported in Table 2. Concentrations of the analysed elements related to their sum varied from 1–6% for winter to 3–13% for summer samples. The W/S ratio calculated for each analysed element varied from 0.06 (Cu) to 1.77 (Br). On average, elemental concentration in summer samples was two times higher when compared with winter samples. This concerns in particular Ca, Ti, Cr, Mn, Fe, Cu and Sr. Main source of these elements could be soil dust and resuspended street dust [10]. In addition, Ca and Ti could originate from cement industry while Fe is strongly linked to steel production. Concentrations of Ca, Fe and Ti strongly correlate (R^2 in the range from 0.95 to 0.97), which suggests their common source. Chlorine was

Table 2. Mean concentrations of selected elements (in $\mu g \cdot g^{-1}$) in the analysed TSPM samples representing summer (S) and winter (W) periods (cf. Table 1)

Element	Concentration [$\mu g \cdot g^{-1}$]		W/S ratio
	Summer (S)	Winter (W)	
Cl	<LLD*	8 400 ± 1 500	n.d.**
K	7 700 ± 1 700	3630 ± 590	0.45 ± 0.13
Ca	16 700 ± 4 030	1760 ± 610	0.11 ± 0.05
Ti	1 280 ± 210	250 ± 50	0.20 ± 0.05
Cr	220 ± 60	65 ± 20	0.29 ± 0.12
Mn	1 070 ± 220	272 ± 74	0.25 ± 0.09
Fe	27 200 ± 5 900	6 800 ± 2 200	0.25 ± 0.10
Cu	4 400 ± 2 500	244 ± 50	0.06 ± 0.03
Zn	3 580 ± 800	2 340 ± 470	0.65 ± 0.20
As	70 ± 20	81 ± 22	1.16 ± 0.46
Br	165 ± 23	293 ± 68	1.77 ± 0.48
Rb	74 ± 17	29 ± 5	0.40 ± 0.12
Sr	160 ± 70	36 ± 3	0.22 ± 0.10
Pb	1 140 ± 230	850 ± 200	0.74 ± 0.23

*Lower limit of detection for Cl is 440 $\mu g \cdot g^{-1}$. **Not determined.

Table 3. The total carbon fraction (TC_{TSPM}) and its carbon isotope composition ($^{14}C_{TSPM}$, $\delta^{13}C_{TSPM}$) in TSPM samples analysed in this study

| Sample code*	TC_{TSPM} [%]	$^{14}C_{TSPM}$** [pMC]	$\delta^{13}C_{TSPM}$ [‰]	FF_{TSPM}*** [%]	FF_{CO2}**** [%]
C-1-S	39.9	62.7	−27.5	43.0 ± 2.6	1.3
C-2-W	41.5	32.8	−24.6	70.2 ± 1.5	5.0
C-3-S	34.8	65.8	−27.0	40.2 ± 2.8	0.7
C-4-W	51.5	26.7	−24.4	75.8 ± 1.2	6.2
C-5-S	37.6	65.5	−26.8	40.5 ± 2.8	0.0
C-6-W	61.4	36.2	−25.1	67.1 ± 1.6	5.0
C-7-S	31.3	56.3	−27.5	48.8 ± 2.4	2.3
C-8-W	44.8	36.6	−25.1	66.7 ± 1.6	5.1
C-9-S	37.8	66.2	−27.6	39.8 ± 2.8	0.8
C-10-W	67.5	34.2	−24.6	68.9 ± 1.5	5.7
C-11-S	45.6	60.0	−26.8	45.5 ± 2.5	2.2
C-12-W	49.2	36.7	−24.8	66.6 ± 1.6	4.1

Notes: The per cent fraction of fossil carbon in TC reservoir (FF_{TSPM}) and per cent fraction of fossil-fuel-derived CO_2 in the local atmosphere of Krakow (FF_{CO2}) are also reported. *Letters W and S signify winter and summer periods, respectively. **Radiocarbon concentration in the analysed TSPM samples expressed in per cent of modern carbon (pMC). ***The reported uncertainty is the combined uncertainty calculated based on Eq. (3). ****Combined uncertainty of FF_{CO2}, calculated based on Eq. (4), is in the order of 0.6%.

observed only in winter samples. The most probable source of this element is maintenance of pavements and roads during winter (de-icing), although combustion of coal and other urban emissions can also introduce Cl to the local atmosphere [10, 12]. The mean Br/Pb ratio varied from 0.15 (summer) to 0.34 (winter). Concentrations of those elements are strongly correlated in summer samples ($R^2 = 0.82$), which suggests transport as an important source of their emissions. Municipal emissions could be additional source of Br leading to the observed increase of mean of Br/Pb ratio during winter [10, 12]. The mean Cu/Pb and Cu/Zn ratios in summer samples were 3.89 and 0.94, respectively. This is in good agreement with the results obtained by Mazzei *et al.* for Genoa (3.9 and 1.1, respectively) [43].

Carbon isotope analyses

The per cent fraction of the TC pool in TSPM samples analysed in this study and its carbon isotope composition are reported in Table 3. The table also contains the values of FF_{TSPM}, the per cent fraction of fossil carbon in the TC reservoir (Eq. (3)) and FF_{CO2}, the per cent fraction of fossil-fuel-derived CO_2 in the local atmosphere of Krakow (Eq. (4)), calculated for the periods covered by TSPM samples. The $^{14}C_{TSPM}$ and $^{13}C_{TSPM}$ values reported in Table 3 are corrected for the presence of calcium carbonate in the analysed TSPM samples (cf. previous sections). As seen in Table 2, the mean concentration of Ca in TSPM samples representing summer periods was ca. 10 times higher than in those representing winter periods. Thus, the resulting corrections were statistically significant only for summer samples. For the fossil fraction of carbon (FF_{TSPM}), they varied between 0.3% and 1.5% (resulting in lower FF_{TSPM} fraction). For $\delta^{13}C_{TSPM}$ the resulting corrections were between 0.2‰ and 0.7‰ (leading to more negative $\delta^{13}C_{TSPM}$ values).

Large contrast between summer and winter percentage contribution of fossil carbon is apparent
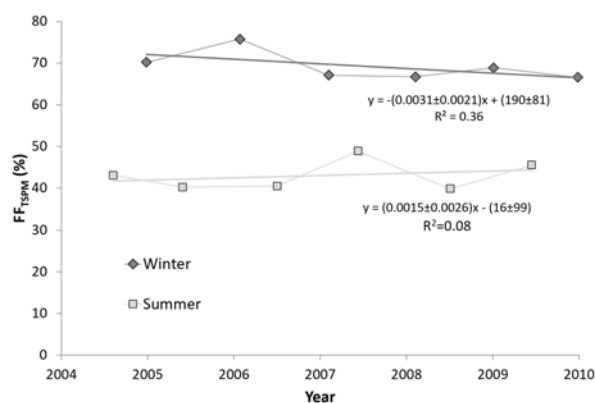
Fig. 3. Temporal variations of fossil-fuel-derived fraction (FF_{TSPM}) of the total carbon reservoir (TC) present in the analysed samples of TSPM.

from Table 3 and Fig. 3. Average FF_{TSPM} values for the analysed period 2004–2010 are (42.9 ± 1.3)% and (69.2 ± 1.3)% for summer and winter samples of TSPM, respectively. These values are substantially higher than those reported by Yttri *et al.* [44] for TC of PM_{10} fraction collected in Oslo, Norway (ca. 27% and 39% for summer and winter samples, respectively). Huang *et al.* [45] reported for Lhasa, Tibet, the range of FF_{TSPM} values from approximately 30% to 65%. Garbaras *et al.* [24] reported FF_{TSPM} values for $PM_{1.0}$ fraction, collected at urban and rural sites in Lithuania, from 32% to 45% and from 18% to 46% for summer and winter seasons, respectively. This large seasonal contrast of FF_{TSPM} values clearly points to additional source of fossil carbon operating in the city during winter time (burning of coal for heating purposes). It is apparent from Fig. 3 that winter FF_{TSPM} values reveal slight decreasing trend in agreement with gradual shift from coal to gas in heating systems of individual households in Krakow.

Figure 4 shows the relationship between fossil-fuel-derived fraction (FF_{TSPM}) of the TC reservoir present in TSPM samples analysed in this study and the percentage contribution of fossil-fuel carbon present in the local atmospheric CO_2 (FF_{CO2}). The
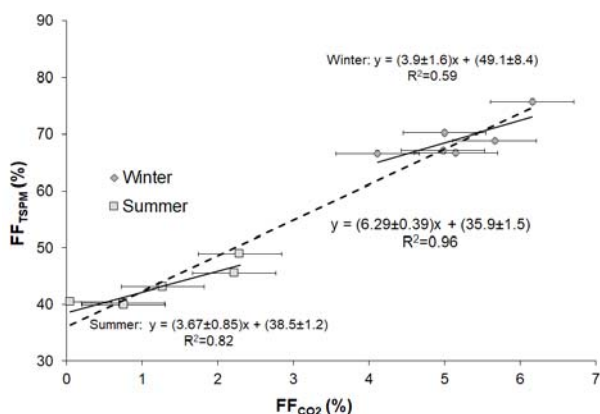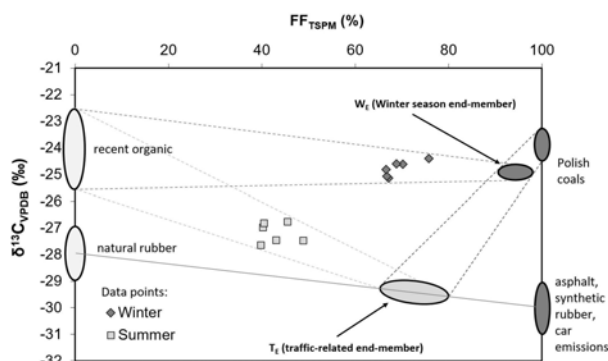
Fig. 4. The relationship between fossil-fuel-derived fraction (FF_{TSPM}) of the total carbon reservoir present in TSPM samples analysed in this study and the percentage contribution of fossil-fuel carbon present in local atmospheric CO_2 (FF_{CO2}).

data points form two distinct clusters representing summer and winter conditions. There is a significant correlation of data within each cluster. Intersects of best fit lines for each data group are ca. 38% and 49% for summer and winter samples, respectively. When all data points are treated as one homogeneous population, reflecting the mean summer–winter contrast in FF_{TSPM} and FF_{CO2} values the resulting intersect is approximately 36%.

In fact, the correlation between FF_{TSPM} and FF_{CO2} is expected as both CO_2 and ^{14}C-free carbon in TSPM are linked with the same emission source, i.e. burning of fossil fuels. Interestingly, the linear fits of the data shown in Fig. 4, when extrapolated to FF_{CO2} equal zero (no fossil carbon in atmospheric CO_2), suggest significant contribution (ca. 36%) of fossil carbon in TC present in the local atmosphere in the form of carbonaceous particles, even if this atmosphere does not contain radiocarbon-free CO_2. This in turn suggests that there are other sources of ^{14}C-free carbon in the local environment during summer season which are not directly linked to burning of fossil fuels. One obvious source of such carbon is mineral fraction of dust (cf. discussion earlier). However, the FF_{TSPM} data shown in Fig. 4 were corrected for its presence. Clearly, another source of such carbon is needed here. This could be for instance wearing of tyres and asphalt pavement of the streets by car traffic.

Combined analysis of ^{13}C and ^{14}C isotope composition of TC reservoir in the investigated TSPM samples allows a deeper insight into the origin of carbon in the investigated samples. The following major sources of carbon should be considered here: (i) burning of coal and wood and its derivatives in individual households in the city for heating purposes, (ii) wearing of tyres and asphalt pavement and (iii) vehicle exhausts. In Fig. 5, δ^{13}C values of TC reservoir in the analysed TSPM samples are plotted as a function of fossil-fuel-derived fraction of carbon in those samples (FF_{TSPM}). Also, the potential sources of carbon present in the analysed samples are marked in Fig. 5 (ovals in the δ^{13}C–FF_{TSPM} space).

Fig. 5. Relationship between ^{13}C isotope composition (δ^{13}C) and fossil-fuel-derived fraction (FF_{TSPM}) in the total carbon reservoir present in TSPM samples analysed in the framework of this study (see text for details).

Modern carbon pool in the TC fraction of the analysed TSPM samples, with the estimated ^{14}C content of (110 ± 5)% of modern carbon ($FF_{TSPM} = 0$, cf. Fig. 5), is a complex reservoir having its roots in at least two major classes sources as far as urban environment is concerned: (i) burning of biomass (mostly wood but also various wood products, such as paper, cardboard, etc.) and (ii) emissions of volatile organic compounds (VOCs) containing carbon by plants. The latter source is active mostly during summer whereas burning of wood and wood products takes place mostly during winter. Plant volatiles can be grouped into isoprenoids or terpenoids, and also oxygenated VOCs such as methanol, acetone, acetaldehyde and others [46]. These volatiles and their derivatives contribute to OC fraction of carbonaceous aerosols. Wood burnt in fireplaces and domestic heating installations originates predominantly from southern Poland. Systematic studies of trees growing in southern Poland revealed the mean δ^{13}C value of the α-cellulose of around –22.5‰, with spread of data (one standard deviation) in the order of 1.5‰ [47]. In a study of larch from central Siberia, Knorre *et al.* [48] reported the mean δ^{13}C values of (-22.40 ± 0.71)‰ for the whole wood and –20.31‰ for the cellulose. If we adopt the above-quoted offset between whole wood and α-cellulose (ca. 2.1‰), then the mean δ^{13}C value of the α-cellulose of trees growing in southern Poland (ca. –22.5‰) can be converted to the mean δ^{13}C value of whole wood (ca. –24.6‰). However, as mentioned earlier, the biomass pool burnt within the city limits also contains paper products (cellulose) which is isotopically enriched with respect to whole wood. Therefore, for the purpose of this study we adopted (-24.0 ± 1.5)‰ as a mean δ^{13}C signature of modern carbon pool in the TC fraction of TSPM samples.

During summer, biogenic VOCs most probably dominate the modern carbon pool. Virtually, nothing is known about ^{13}C isotope composition of biogenic VOCs. Kornilova *et al.* [49] reported δ^{13}C values of ambient aromatic VOCs (benzene, toluene, ethyl benzene, σ-xylene, *p,m*-xylene) measured in Toronto, Canada in 2009 and 2010, ranging from –23.3‰ to –25.0‰. Thus we adopted the same mean value of (-24.0 ± 1.5)‰ as δ^{13}C signature of modern carbon pool in the TC fraction of TSPM during summer.

The third source of modern carbon in the analysed TC fraction is natural rubber which is present in car tyres. Modern car tyres are complex, multicomponent products. According to the available data, they contain 15–25% of natural rubber and approximately the same percentage of synthetic rubber. A dedicated study has shown that trunk latex which is the basic substrate for natural rubber has $\delta^{13}C$ values in the range of –27‰ to –29‰ [50].

Several sources contribute to ^{14}C-free carbon pool ($FF_{TSPM} = 100\%$; cf. Fig. 5) in the TC fraction of the analysed TSPM samples: (i) burning of coal for heating purposes, (ii) car emissions (mainly soot particles from diesel engines), (iii) wearing of tyres (synthetic rubber, soot, black carbon, oil, other petrochemicals) and (iv) wearing of asphalt pavement. ^{13}C isotope composition of Polish hard coals falls in a relatively narrow range from approximately –23.3‰ to –24.5‰ [51]. In a comprehensive study, Widory [52] has shown that ^{13}C isotope composition of liquid fuels (diesel, unleaded and regular gasoline, fuel oil, heavy fuel) varies in a relatively narrow range from approximately –27‰ to –30‰. He reported that combustion particles from diesel engines are slightly enriched with respect to liquid fuel (by ca. 1.2‰) whereas CO_2 emitted by car exhausts is depleted in ^{13}C roughly by the same magnitude. A study of carbon isotope composition of CO_2 emitted by various types of cars (e.g. diesel and gasoline engines with or without catalyst and LPG engines with or without catalyst) conducted within the Krakow metropolitan area [53] revealed $\delta^{13}C$ values in the range from –29‰ to –32‰ [53]. Mašalaitė *et al.* [54] reported that the mean $\delta^{13}C$ value of diesel and gasoline fuel produced from oil of Russian origin is $(-31.3 \pm 0.1)‰$. Since fuel available in Poland is predominantly of Russian origin, the above quoted offset between liquid fuel and combustion particles of 1.2‰ can be used to derive mean $\delta^{13}C$ signature of ^{14}C-free carbon pool of approximately –30.0‰ associated with car emissions in Krakow. Carbon isotope composition of asphalt which could be of natural or synthetic origin resembles that of crude oil. In Poland, exclusively synthetic asphalt produced from crude oils of Russian origin is on the market ($\delta^{13}C = (-31.3 \pm 0.1)‰$). On the other hand, car tyres in Poland originate nowadays predominantly from the global market and synthetic rubber that is one of the components of those tyres can be enriched with respect to crude oil of Russian origin [52, 54]. Thus, for the purpose of semi-quantitative assessment of carbon sources contributing to TC pool in TSPM samples analysed in this study, we adopt the $\delta^{13}C$ value of $(-30.0 \pm 1.0)‰$ as a mean signature of ^{14}C-free carbon pool associated with car traffic in the city.

Traffic-related endmember (T_E) marked by oval in Fig. 5 consists of carbonaceous particles associated with wearing of tyres and asphalt pavement as well as particles emitted by car engines. Since the intensity of traffic does not change significantly with season, the assumption about stable position of this endmember in the $\delta^{13}C_{TSPM}$–FF_{STPM} space is justified.

If the position of traffic-related endmember in the $\delta^{13}C_{TSPM}$–FF_{STPM} space does not change significantly with season, it is possible to reconstruct graphically the position of winter season endmember (W_E) with additional constraint that the data points for summer and winter should lie within the respective mixing spaces. During summer, traffic-related endmember mixes with recent OC pool (mostly biogenic emissions; cf. discussion earlier). During winter season, a strong source of carbonaceous particles related to burning of coal for heating purposes comes into play and mixes with traffic-related endmember (T_E), thus defining winter season endmember (W_E) which then mixes up with recent OC pool (mostly burning of wood and its derivatives for heating purposes; cf. discussion earlier).

The mixing scenario presented in Fig. 5 allows a semi-quantitative assessment of the contribution of T_E and W_E pools in the samples of TSPM analysed in the framework of this study. During summer, the contribution of T_E endmember to the TC present in the analysed TSPM samples is approximately 61%. During winter season, the W_E pool contributes approximately 74%. The W_E pool is composed of carbonaceous particles associated with coal burning (ca. 80%) and particles belonging to traffic-related endmember (20%).

Conclusions

The pilot study of TSPM collected in Krakow atmosphere between 2004 and 2010, representing summer and winter conditions, revealed large seasonal variability of carbon isotope composition of the TC pool present in the analysed TSPM samples. This large variability generally reflects seasonally varying contribution of different sources of fossil and modern carbon to the TC pool. The elemental composition of TSPM also reveals distinct seasonal variability of the analysed elements, reflecting varying mixture of natural and anthropogenic sources of those elements during winter and summer seasons.

The percentage contribution of fossil carbon to the TC pool in the analysed TSPM samples fluctuated around 43% for samples collected during summer season and it increased to 66–76% during winter season. Such high loads of fossil carbon in carbonaceous aerosols were generally not observed for other urban locations being studied.
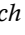
This study revealed strong linear relationship between the fossil carbon load in the analysed TSPM samples and the fossil carbon load in the local atmospheric CO_2. In fact, such link was expected as both atmospheric CO_2 and ^{14}C-free carbon in TSPM are associated with the same emission source, i.e. burning of fossil fuels. Interestingly, extrapolation of this relationship to the atmospheric CO_2 totally devoid of fossil carbon still leaves significant contribution of fossil carbon (ca. 38%) in the TC present in local atmosphere in the form of carbonaceous aerosols. This points to the presence of additional sources of carbonaceous particles containing fossil carbon in the city atmosphere, but not associated with burning of fossil fuels. Wearing of tyres and asphalt pavement associated with car traffic in the city is most probably the main source of such particles.

Combining radioactive and stable carbon isotope composition of TC fraction in the investigated TSPM samples allowed a deeper insight into the origin of carbon in carbonaceous aerosols present in the urban environment and a semi-quantitative partitioning of different sources of carbon such as recent biogenic carbon, fossil carbon from burning of coal and other fossil fuels, recent and fossil carbon from wearing of car tyres and asphalt pavement.

ORCID

J. Bartyzel http://orcid.org/0000-0001-8163-2680
Z. Gorczyca http://orcid.org/0000-0002-1643-4589
K. Rozanski http://orcid.org/0000-0003-4704-0379
L. Samek http://orcid.org/0000-0001-8636-2771
M. Zimnoch http://orcid.org/0000-0002-0594-9376

References

1. Baklanov, A., Molina, L. T., & Gauss, M. (2016). Megacities, air quality and climate. *Atmos. Environ., 126*, 235–249. DOI: 10.1016/j.atmosenv.2015.11.059.

2. World Human Organization. (2016). *Urban Ambient Air Pollution database – Update 2016.* Retrieved August 20, 2019, from www.who.int/airpollution/data/cities-2016/en/.

3. Molina, L. T., Madronich, S., Gaffney, J. S., Apel, E., de Foy, B., Fast, J., Ferrare, R., Herndon, S., Jimenez, J. L., Lamb, B., Osornio-Vargas, A. R., Russell, P., Schauer, J. J., Stevens, P. S., Volkamer, R., & Zavala, M. (2010). An overview of the MILAGRO 2006 Campaign: Mexico City emissions and their transport and transformation. *Atmos. Chem. Phys., 10*, 8697–8760. DOI: 10.5194/acp-10-8697-2010.

4. Guo, S., Hu, M., Zamora, M. L., Peng, J., Shang, D., Zheng, J., Du, Z., Wu, Z., Shao, M., Zeng, L., Molina, M. J., & Zhang, R. (2014). Elucidating severe urban haze formation in China. *PNAS, 111*(49), 17373–17378. DOI: 10.1073/pnas.1419604111.

5. Zou, Y., Wang, Y., Zhang, Y., & Koo, J. -H. (2017). Arctic sea ice, Eurasia snow, and extreme winter haze in China. *Sci. Adv., 3*(3), e1602751. DOI: 10.1126/sciadv.1602751.

6. Fang, G. -C., Wu, Y. -S., Huang, S. -H., & Rau, J. -Y. (2005). Review of atmospheric metallic elements in Asia during 2000–2004. *Atmos. Environ., 39*(17), 3003–3013. DOI: 10.1016/j.atmosenv.2005.01.042.

7. Rodriguez, S., Querol, X., Alastuey, A., & la Rosa, J. D. (2007). Atmospheric particulate matter and air quality in the Mediterranean: a review. *Environ. Chem. Lett., 5*(1), 1–7. DOI: 10.1007/s10311-006-0071-0.

8. Cuccia, E., Massabo, D., Ariola, V., Bove, M. C., Fermo, P., Piazzalunga, A., & Prati, P. (2013). Size-resolved comprehensive characterization of airborne

9. particulate matter. *Atmos. Environ., 67*, 14–26. DOI: 10.1016/j.atmosenv.2012.10.045.

9. Lammel, G., Rohrl, A., & Schreiber, H. (2002). Atmospheric lead and bromine in Germany. Post abatement levels, variabilities and trends. *Environ. Sci. Pollut. Res., 9*(6), 397–404. DOI: 10.1007/BF02987589.

10. Vallius, M., Janssen, N. A. H., Heinrich, J., Hoek, G., Ruuskanen, J., Cyrys, J., Van Grieken, R., de Hartog, J. J., Kreyling, W. G., & Pekkanen, J. (2005). Sources and elemental composition of ambient PM2.5 in three European cities. *Sci. Total Environ., 337*(1/3), 147–162. DOI: 10.1016/j.scitotenv.2004.06.018.

11. Pant, P., & Harrison, R. M. (2013). Estimation of the contribution of road traffic emissions to particulate matter concentrations from field measurements. A review. *Atmos. Environ., 77*, 78–97. DOI: 10.1016/j.atmosenv.2013.04.028.

12. Chueinta, W., Hopke, P. K., & Paatero, P. (2000). Investigation of sources of atmospheric aerosol at urban and suburban residential areas in Thailand by positive matrix factorization. *Atmos. Environ., 34*(20), 3319–3329. DOI: 10.1016/S1352-2310(99)00433-1.

13. Amato, F., Alastuey, A., Karanasiou, A., Lucarelli, F., Nava, S., Calzolai, G., Severi, M., Becagli, S., Gianelle, V. L., Colombi, C., Alves, C., Custodio, D., Nunes, T., Cerqueira, M., Pio, C., Eleftheriadis, K., Diapouli, E., Reche, C., Cruz Minguillon, M., Manousakas, M. I., Maggos, T., Vratolis, S., Harrison, R. M., & Querol, X. (2016). AIRUSE-LIVE+: a harmonized PM speciation and source apportionment in five southern European cities. *Atmos. Chem. Phys., 16*, 3289–3309. DOI: 10.5194/acp-16-3289-2016.

14. Samek, L., Stegowski, Z., Furman, L., Styszko, K., Szramowiat, K., & Fiedor, J. (2017). Quantitative assessment of PM2.5 sources and their seasonal variation in Krakow. *Water Air Soil Pollut., 228*, 290. DOI: 10.1007/s11270-017-3483-5.

15. Chow, J. C., Watson, J. G., Crow, D., Lowental, D. H., & Merrifield, T. (2001). Comparison of IMPROVE and NIOSH carbon measurements. *Aerosol Sci. Technol., 34*(1), 23–34. DOI: 10.1080/02786820119073.

16. Górka, M., Rybicki, M., Simoneit, B. R. T., & Marynowski, L. (2014). Determination of multiple organic matter sources in aerosol PM10 from Wrocław, Poland using molecular and stable carbon isotope compositions. *Atmos. Environ., 89*, 739–748. DOI: 10.1016/j.atmosenv.2014.02.064.

17. Aguilera, J., & Whigham, L. D. (2018). Using the $^{13}C/^{12}C$ isotope ratio to characterize the emission sources of airborne particulate matter: a review of literature. *Isot. Environ. Health Stud., 54*(6), 573–587. DOI: 10.1080/10256016.2018.1531854.

18. Currie, L. A. (2000). Evolution of multidisciplinary frontiers of ^{14}C aerosol science. *Radiocarbon, 42*(1), 115–126. DOI: 10.1017/S003382220005308X.

19. Heal, M. R. (2014). The application of carbon-14 analyses to the source apportionment of atmospheric carbonaceous particulate matter: a review. *Anal. Bioanal. Chem., 406*, 81–98. DOI: 10.1007/s00216-013-7404-1.

20. Szidat, S., Jenk, T., Gäggeler, H., Synal, H. -A., Fisseha, R., Baltensperger, U., Kalberer, M., Samburova, V., Reimann, S., Kasper-Giebl, A., & Hajdas, I. (2004). Radiocarbon (^{14}C)-deduced biogenic and anthropogenic contributions to organic carbon

(OC) of urban aerosols from Zürich, Switzerland. *Atmos. Environ.*, *38*, 4035–4044. DOI: 10.1016/j.atmosenv.2004.03.066.

21. Zotter, P., El-Haddad, I., Zhang, Y., Hayes, P. L., Zhang, X., Lin, Y. -H., Wacker, L., Schnelle-Kreis, J., Abbaszade, G., Zimmermann, R., Surratt, J. D., Weber, R., Jimenez, J. L., Szidat, S., Baltensperger, U., & Prévôt, A. S. H. (2014). Diurnal cycle of fossil and nonfossil carbon using radiocarbon analyses during CalNex. *J. Geophys. Res. Atmos.*, *119*, 6818–6835. DOI: 10.1002/2013JD021114.

22. Zhang, Y. -L., Huang, R. -J., El Haddad, I., Ho, K. -F., Cao, J. -J., Han, Y., Zotter, P., Bozzetti, C., Daellenbach, K. R., Canonaco, F., Slowik, J. G., Salazar, G., Szwikowski, M., Schnelle-Kreis, J., Abbaszade, G., Zimmermann, R., Baltensperger, U., Prévôt, A. S. H., & Szidat, S. (2015). Fossil vs. non-fossil sources of fine carbonaceous aerosols in four Chinese cities during the extreme winter haze episode of 2013. *Atmos. Chem. Phys.*, *15*, 1299–1312. DOI: 10.5194/acp-15-1299-2015.

23. Dusek, U., Hitzenberger, R., Kasper-Giebl, A., Kistler, M., Meijer, H. A. J., Szidat, S., Wacker, L., Holzinger, R., & Röckmann, T. (2017). Sources and formation mechanisms of carbonaceous aerosol at a regional background site in the Netherlands: insights from a year-long radiocarbon study. *Atmos. Chem. Phys.*, *17*, 3233–3251. DOI: 10.5194/acp-17-3233-2017.

24. Garbaras, A., Šapolaitė, J., Garbarienė, I., Ežerinskis, Z., Mašalaite-Nalivaikė, A., Skipitytė, R., Plukis, A., & Remeikis, V. (2018). Aerosol source (biomass, traffic and coal emission) apportionment in Lithuania using stable carbon and radiocarbon analysis. *Isot. Environ. Health Stud.*, *54*(5), 463–474. DOI: 10.1080/10256016.2018.1509074.

25. Samek, L. (2012). Source apportionment of the PM10 fraction of particulate matter collected in Krakow, Poland. *Nukleonika*, *57*(4), 601–606.

26. Samek, L., Zwozdziak, A., & Sowka, I. (2013). Chemical characterization and source identification of Particulate Matter PM10 in a rural and an urban site in Poland. *Environ. Prot. Eng.*, *39*(4), 91–103. DOI: 10.5277/epe130408.

27. World Health Organization. (2005). *WHO Air quality guidelines for particulate matter, ozone, nitrogen dioxide and sulfur dioxide. Global update 2005. Summary of risk assessment*. WHO.

28. European Union. (2008). Directive 2008/50/EC of the European Parliament and of the Council of 21 May 2008 on ambient air quality and cleaner air for Europe. *Official Journal of the European Union*, 11.6.2008, L 152. Available from https://eur-lex.europa.eu/legal-content/en/ALL/?uri=CELEX%3A32008L0050.

29. Chief Inspectorate of Environmental Protection. (2017). *Air quality portal – PM10 data from Krakow; Air quality stations for the period 2005–2015*. Warszawa: CIEP. Retrieved July 30, 2019, from http://powietrze.gios.gov.pl. (in Polish).

30. Bajorek-Zydroń, K., & Wężyk, P. (Eds.). (2016). *Atlas pokrycia terenu i przewietrzania Krakowa (Atlas of land cover and ventilation of Krakow)*. Krakow: Urząd Miasta Krakowa. Available from http://geo.ur.krakow.pl/download/pobierz.php?file=publikacje/literatura/Wezyk_Atlas_2016_tekst.pdf.

31. Statistical Office of Poland. (2017). *Statistical Office of Poland information portal – Transport and communication in Kraków; vehicles*. Retrieved July 30, 2019, from http://bdl.stat.gov.pl. (in Polish).

32. Zimnoch, M., Wach, P., Chmura, L., Gorczyca, Z., Rozanski, K., Godlowska, J., Mazur, J., Kozak, K., & Jeričević, A. (2014). Factors controlling temporal variability of near-ground atmospheric ^{222}Rn concentration over central Europe. *Atmos. Chem. Phys.*, *14*(18), 9567–9581. DOI: 10.5194/acp-14-9567-2014.

33. Holynska, B., Najman, J., Ostachowicz, B., Ostachowicz, J., Trabska, J., & Wegrzynek, D. (1996). Analytical application of multifunctional system of EDXRF. *J. Trace Microprobe Tech.*, *14*(1), 119–130.

34. Vekemans, B., Janssens, K., Vincze, L., Adams, F., & Van Espen, P. (1994). Analysis of X-ray spectra by iterative least squares (AXIL). New developments. *X-Ray Spectrom.*, *23*(6), 278–285. DOI: 10.1002/xrs.1300230609.

35. Major, I., Furu, E., Janovics, R., Hajdas, I., Kertész, Zs., & Molnár, M. (2012). Method development for the ^{14}C measurement of atmospheric aerosols. *Acta Phys. Debrecina*, *XLVI*, 83–95.

36. Mook, W. G., & van der Plicht, J. (1999). Reporting ^{14}C activities and concentrations. *Radiocarbon*, *41*(3), 227–239. DOI: 10.1017/S0033822200057106.

37. Kuc, T., Rozanski, K., Zimnoch, M., Necki, J., Chmura, L., & Jelen, D. (2007). Two decades of regular observations of $^{14}CO_2$ and $^{13}CO_2$ content in atmospheric carbon dioxide in central Europe: long-term changes of regional anthropogenic fossil fuel CO_2 emissions. *Radiocarbon*, *49*(2), 807–816. DOI: 10.1017/S0033822200042685.

38. Kuc, T. (1991). Concentration and carbon isotopic composition of atmospheric CO_2 in southern Poland. *Tellus B*, *43*(5), 373–378. DOI: 10.3402/tellusb.v43i5.15411.

39. Florkowski, T., Grabczak, J., Kuc, T., & Rozanski, K. (1975). Determination of radiocarbon in water by gas or liquid scintillation counting. *Nukleonika*, *20*(11/12), 1053–1066.

40. Levin, I., Schuchard, J., Kromer, B., & Münnich, K. O. (1989). The continental European Suess effect. *Radiocarbon*, *31*(3), 431–440. DOI: 10.1017/S0033822200012017.

41. Levin, I., Naegler, T., Kromer, B., Diehl, M., Francey, R., Gomez-Pelaez, A., Steele, P., Wagenbach, D., Weller, R., & Worthy, D. (2010). Observations and modeling of the global distribution and long-term trend of atmospheric $^{14}CO_2$. *Tellus B*, *62*(1), 26–46. DOI: 10.1111/j.1600-0889.2009.00446.x.

42. Zimnoch, M., Jelen, D., Galkowski, M., Kuc, T., Necki, J., Chmura, L., Gorczyca, Z., Jasek, A., & Rozanski, K. (2012). Partitioning of atmospheric carbon dioxide over Central Europe: insights from combined measurements of CO_2 mixing ratios and their carbon isotope composition. *Isot. Environ. Health Stud.*, *48*(3), 421–433. DOI: 10.1080/10256016.2012.663368.

43. Mazzei, F., D'Alessandro, A., Lucarelli, F., Nava, S., Prati, P., Valli, G., & Vecchi, R. (2008). Characterization of particulate matter sources in an urban environment. *Sci. Total Environ.*, *401*(1/3), 81–89. DOI: 10.1016/j.scitotenv.2008.03.008.

44. Yttri, K. E., Simpson, D., Stenström, K., Puxbaum, H., & Svendby, T. (2011). Source apportionment of the

carbonaceous aerosol in Norway – quantitative estimates based on ^{14}C, thermal-optical and organic tracer analysis. *Atmos. Chem. Phys.*, *11*(17), 9375–9394. DOI: 10.5194/acp-11-9375-2011.

45. Huang, J., Kang, S., Shen, C., Cong, Z., Liu, K., Wang, W., & Liu, L. (2010). Seasonal variations and sources of ambient fossil and biogenic-derived carbonaceous aerosols based on ^{14}C measurements in Lhasa, Tibet. *Atmos. Res.*, *96*(4), 553–559. DOI: 10.1016/j.atmosres.2010.01.003.

46. Vivaldo, G., Masi, E., Taiti, C., Caldarelli, G., & Mancuso, S. (2017). The network of plants volatile organic compounds. *Sci. Rep.*, *7*, 11050. DOI: 10.1038/s41598-017-10975-x.

47. Sensuła, B., & Pazdur, A. (2013). Stable carbon isotopes of glucose received from pine tree-rings as bioindicators of local industrial emission of CO_2 in Niepołomice Forest (1950–2000). *Isot. Environ. Health Stud.*, *49*(4), 532–541. DOI: 10.1080/10256016.2013.865026.

48. Knorre, A. A., Siegwolf, R. T. W., Saurer, M., Sidorova, O. V., Vaganov, E. A., & Kirdianov, A. V. (2010). Twentieth century trends in tree ring stable isotopes (δ^{13}C and δ^{18}O of *Larix sibirica* under dry conditions in the forest steppe in Siberia. *J. Geophys. Res.*, *115*(G3), G03002. DOI: 10.1029/2009JG000930.

49. Kornilova, A., Huang, L., Saccon, M., & Rudoplh, J. (2016). Stable carbon isotope ratios of ambient aromatic volatile organic compounds. *Atmos. Chem. Phys.*, *16*(18), 11755–11772. DOI: 10.5194/acp-16-11755-2016.

50. Kanpanon, N., Kesemsap, P., Thaler, P., Kositsup, B., Gay, F., Lacote, R., & Epron, D. (2015). Carbon isotope composition of latex does not reflect temporal variations of photosynthetic carbon isotope discrimination in rubber trees (*Hevea brasiliensis*). *Tree Physiol.*, *35*(11), 1166–1175. DOI: 10.1093/treephys/tpv070.

51. Lewan, M. D., & Kotarba, M. J. (2014). Thermal-maturity limit for primary thermogenic-gas generation from humic coals as determined by hydrous pyrolysis. *AAPG Bull.*, *98*, 2581–2610. DOI: 10.1306/06021413204.

52. Widory, D. (2006). Combustibles, fuels and their combustion products: A view through carbon isotopes. *Combust. Theory Model.*, *10*(5), 831–841. DOI: 10.1080/13647830600720264.

53. Zimnoch, M. (2009). Stable isotope composition of carbon dioxide emitted from anthropogenic sources in the Krakow region. *Nukleonika*, *54*(4), 291–295.

54. Mašalaitė, A., Garbaras, A., & Remeikis, V. (2012). Stable isotopes in environmental investigations. *Lith. J. Phys.*, *52*(3), 261–268.